JOURNAL OF SANDWICH STRUCTURES & MATERIALS

Standard Article

Journal of Sandwich Structures & Materials
2023, Vol. 0(0) 1–32

DOI: 10.1177/10996362231170405
journals.sagepub.com/home/jsm
SAGE

Mechanical behaviour of fabric-reinforced plastic sandwich structures: A state-of-the-art review

Norman Osa-uwagboe[1,2], Vadim V Silberschimdt[1], Adedeji Aremi[3] and Emrah Demirci[1]

Abstract

The use of fibre-reinforced plastics (FRPs) in sandwich structures increased for various industrial applications thanks to their strength-to-weight ratio which provides designers with advanced options for modern structures. FRP Sandwich Structures (FRPSS) are often used in aerospace, biomedical, defence, and marine products, where their high structural performance is required to sustain complex in-service loads and withstand varying environmental conditions. Progressive degradation of FRPSS under such circumstances has been a subject of interest for researchers owing to safety requirements for products with FRP. This paper reviews the state-of-the-art of the mechanical behaviour of FRPSS subjected to various loading regimes. It highlights the variation in structural performance, viscoelastic properties, damage resistance, and sequence of environmental degradation of FRPSS. Numerical methods and damage algorithms used to predict failures are also presented to provide sufficient knowledge for the design of FRPSS. This review contributes to further research on characterizing the properties of FRPSS under quasi-static and dynamic loading conditions.

Keywords

Fibre-reinforced plastics, sandwich structures, finite element analysis, damage, environmental degradation

[1]Wolfson School of Mechanical, Electrical, and Manufacturing Engineering, Loughborough University, Loughborough, UK
[2]Air Force Research and Development Centre, Nigerian Air Force Base, Kaduna, Nigeria
[3]School of Mechanical Engineering, Coventry University, Coventry, UK

Corresponding author:
Emrah Demirci, Wolfson School of Mechanical, Electrical, and Manufacturing Engineering, Loughborough University, Epinal Way, Loughborough LE11 3TU, UK.
Email: E.demirci@lboro.ac.uk

Introduction

Fibre-reinforced plastics (FRPs) are composite materials containing fibres embedded in a polymer matrix; they are non-homogeneous and anisotropic. The last five decades have witnessed a rapid increase in the exploitation of FRPs in industrial applications, thanks to their superior performance compared to traditional metals and alloys.[1] While offering a high stiffness-to-wight ratio, in service, they retain a significant level of resistance to corrosion and fatigue, which elongates the life span of products made of FRPs. Their properties can also be tailored to meet the requirements of specific applications especially by adapting features of fibres and by changing the volume fraction and orientation of fibres.[2] Recent advances in FRP design are related to sandwich structures made with FRPs laminate face sheets to optimize their weight without compromising the structural performance. Composite sandwich structures consist of multiple layers of materials joined into a single structure to efficiently support the load transfer between the constituent. FRPSS are particularly exploited in cases requiring high bending stiffness at low weight. For instance, it is common to find sandwich structures in applications such as automotive and aerospace applications, wind turbines, naval vessels, boats, refrigeration trailers, rail cars, and bridge construction.[3–5] The overall performance of sandwich structures depends on the properties of their components and the quality of joining. The research in[6,7] adapted the constituents of sandwich structures to certain engineering applications.

FRP sandwich face sheets primarily resist normal stresses under bending while providing enhanced fatigue and damping properties. FRPSS are usually designed with relatively thin sheets in comparison to the core which is often much thicker to provide sufficient stiffness in compressive, tensile, bending, and buckling loadings.[8] Face sheets of carbon-fibre-reinforced plastics (CFRP) and glass-fibre-reinforced plastics (GFRP) in FRPSS (Figure 1) are often tailored for specific applications. The core of the sandwich provides resistance to shear stresses and extension in the thickness direction.[9] Generally, sandwich structures are made with cores of lower density compared to the face sheets to maximize the stiffness-to-weight ratio. The selection of face sheets and core materials could be guided by several parameters such as application, operational environment, and stiffness requirement. A common selection criterion used in choosing FRP face sheets is Ashby's[10] material property guideline. In recent years, there have been advancement in the use of a wide range of fabric designs as face sheets for FRPSS, some of which include the use FRP fabrics kitted in the weft and warp directions. These fabrics have demonstrated significant improvement in the mechanical properties of the modified structures when compared to more traditional constituents.[11,12] The mechanical characteristics of materials commonly used as face sheets in FRPSS is given in Table 1 below.

Sandwich cores are commonly made from metallic and non-metallic materials such as balsa wood, truss core, and various type of synthetic foams such as Polyvinyl chloride (PVC) and Polyethylene terephthalate (PET), honeycomb cores made from metals such as Aluminium or nonmetals such as Nomex.[14–17] The mechanical characteristics of some of the commonly used cores in FRPSS are described in Table 2.

An example of the typical constituents of an FRPSS is described in Figure 2. A detailed analysis of the calculation of the stiffness and strength of constituents of sandwich structures is given in Carlsson.[25]

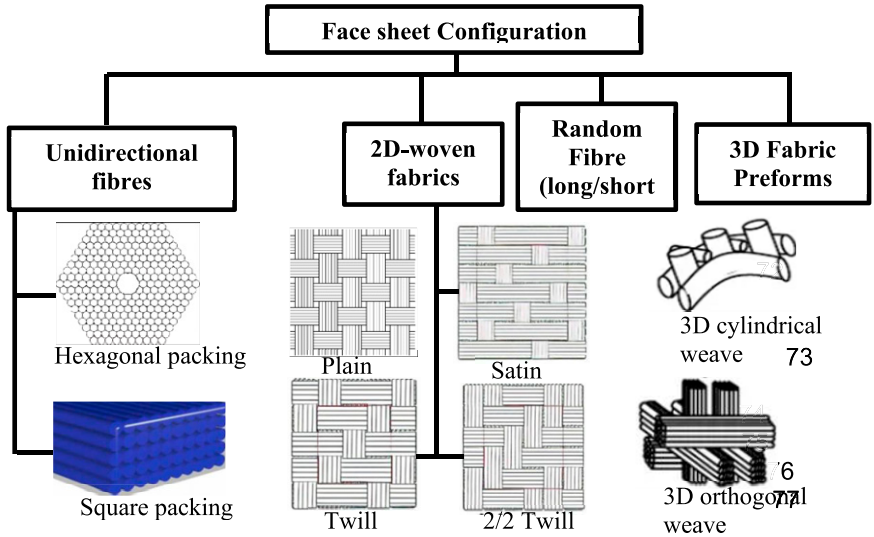

Figure 1. Common FRP face sheet geometry.

Table 1. Mechanical properties of common face sheets of FRPSS.[13]

	Mechanical properties				
Fibre	Density (kg/m^3)	Elastic modulus (GPa)	Elastic strength (GPa)	Max strain (%)	Specific stiffness (E/ρ)
E-glass	2.58	69.72	3.5–3.8	4.5–4.9	28
Carbon HS	1.8	160–250	1.4–4.9	0.8–1.9	139
Carbon IM	1.75	276–317	2.35–7.0	0.8–2.2	181
Carbon HM	1.8	338–436	1.9–5.5	0.5–1.4	242
Carbon UHM	1.9	440–827	1.8–3.5	0.4–0.5	435
Aramid K-49	1.45	131	3.6–4.1	2.8	90
PE $_{Sp\ 900}$	0.97	117	2.6	3.5	120
SiC	3.0	45–480	0.3–4.9	0.6–1	160
Flax	1.4	60–95	0.5–1.6	1.5–3	67

Specific features of FRP necessitated investigations into their performance when subjected to a diverse range of loads and environmental conditions.[26–28] Various studies elucidated the effects of manufacturing techniques and the configuration of their constituent parts on the mechanical properties of the structures.[29–35] Particularly their behaviour under low-velocity impacts such as bird strikes, hailstones, or lightning strikes as well as common maintenance and manufacturing operations was studied extensively.

Table 2. Mechanical properties of common cores of FRPSS.

Core type	Mechanical properties				Ref
	Density (kg/m^3)	Elastic modulus (GPa)	Shear modulus (GPa)	Elastic strength (MPa)	
Wood	370	1.36	3.34	69.72	18
PET	150	0.80[c]	0.29	2.5	19
PVC	65	0.8	0.2	1.8	20
Aluminium honeycomb	2.72	70	0.27	27	21
Nomex honeycomb	3.2	01.96	0.17	64.2	22
Polyurethane foam	48	0.93	0.13	0.45	23
Polymethacrylmide (PMI)	75	0.029	0.29	2.8	24

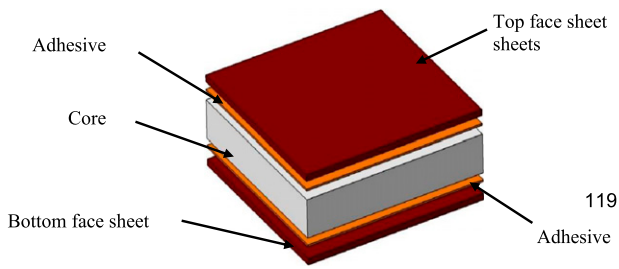

Figure 2. Constituents of a typical composite sandwich structure.

Under such accidents, the mechanical performance of the FRPSS could be compromised in-service potentially leading to a reduced life.[36] This can be exacerbated by the in-visibility of sub-surface progressive damage and adverse environmental conditions. This is often associated with a so-called *barely visible damage* that can compromise the residual strength of the structure. This led to the investigation of several failure modes including indentation/cracking, face sheet buckling, delamination within the face sheet, and disbonding between the face sheet and the core.[37–39] Research conducted in this area can be classified into three main fields; experimental,[40,41] numerical,[42] and non-destructive test methods (NDTs).[19,43,44]

This review presents the findings of recent experimental and numerical studies on the performance of FRPSS subjected to quasi-static and dynamic loading with or without environmental degradation. This paper reviews recent data on the mechanical properties of FRPSS. Selected experimental and numerical studies covering the elastoplastic and viscoelastic behaviours of the constituents of the structure under quasi-static and dynamic loads are discussed. Finally, future directions for the research into FRPSS are outlined. This paper aims to provide an up-to-date understanding of the state-of-the-art of FRPSS to enable researchers rapidly gain insights to support their future research. It also highlights

the emerging areas in the literature on the mechanics of FRPSS that may require further research. The selected research highlighted in this article is focused on recent studies in the literature from 2007 to 2022 that highlight the quasi-static and visco-elastic behavior, numerical simulation, and environmental degradation of FRPSS.

Experimental analysis

Experimental investigations of the mechanical properties of FRPSS abound in the literature, especially on their elastic and damage behaviour. Several studies[45–48] used different experimental techniques to understand the nature of damage of FRPSS.

Characterization of quasi-static mechanical behaviour

In analysing of mechanical properties of sandwich structures, variations in their parameters such as stacking sequence of face sheets, core density, and interfacial bonding between the core and the face sheet are vital in determining the damage resistance and damage tolerance of the structure.[49–58] For instance, Xie et al.[59] investigated the mechanical behaviour of FRPSS with a hybrid core made from polyurethane foam of different densities, impregnated with galvanized metal tooth nails, by subjecting them to three-point bending and double-cantilever-beam tests. The research compared strengthened sandwich samples with galvanized metal tooth nails between the E-glass face sheets and the polyurethane foam core with that without such nails. Results showed that increasing the core density from 35 kg/m^3 to 159 kg/m^3, increased the peak strength of the samples by 90%. Similarly, an increase in the face sheet and PET foam thickness can significantly enhance the ultimate flexural load of the panels. For instance, an increase in the face sheet thickness from 3 mm to 4.5 mm and core thickness from 40 mm to 80 mm resulted in the rise of the ultimate flexural load by 88.9% and 115.6%, respectively.[19] This enforces the fact that a thicker web core can enhance the bending properties of sandwich panels; however, this could reduce their weight-to-stiffness ratio. Additionally, this research identified the main failure modes of FRP sandwich lattice-web panels as core shear, top face sheet compression, and skin/core local debonding. Similar studies on the flexural properties of FRPSS with different constituents were carried out.[18,19,56,60–64] For example, Sayahlatifi et al.,[60] investigated the flexural properties of e-glass/epoxy panels with the inclusion of corrugated composites in the balsa-wood core. They revealed an increase in the post-failure regime of the load-displacement response. Furthermore, it was observed that while the hybrid core increased the strength and stiffness of the sandwich structure (by 78.1% and 29%, respectively), it had a minimal effect on the stiffness-to-weight ratio. Interestingly, Xie et al.[19] established that the use of lattice web (the inclusion of layers of reinforcements along the through-thickness direction of the core at designated intervals) and PET foams prevented the complete failure of the structure even after the onset of damage. Also, the increase in the thickness of the face sheets can alter the failure mode of the structure from compression rupture of face sheets to skin/core debonding.

Adigun et al.[65] investigated the mechanical performance of FRPSS by comparing the effects of hybrid (natural/synthetic) reinforcements and fully natural or synthetic face sheets.

In the study, FRPSS with core made from syntactic foam filled with hollow glass microspheres and kenaf/GFRP/epoxy face sheets were used. The study showed that the specimens with hybrid face sheets (kenaf/glass arrangement) had the highest compressive strength while another hybrid arrangement - glass/kenaf - of face sheets performed better under flexural loading conditions as shown in Figure 3. This was attributed to the contributions of the various constituents and their demonstrated adhesive interaction force. Such enhanced properties could be beneficial for industry-specific applications such as the design of marine and aerospace structures.

A breakdown of some features of elastic-plastic behaviour of composite sandwich panels inferred from various studies is presented in Table 3.

Characterization of the visco-elastic performance

Composite sandwich structures like many composites exhibit viscoelastic behaviour under a time-dependent load condition that cause the structure to experience creep or stress relaxation. The dynamic mechanical analysis (DMA) test is often used to assess the viscoelastic properties of composite experiencing such conditions. This test investigates the material response in terms of parameters such as storage modulus, loss modulus, and tan δ of materials and structures within specific temperature and frequency ranges.[71,72] The low load capabilities of most measuring equipment have minimized the quantity of data for the frequency range (0 Hz–150 Hz). Redmann et al.[73] compared the relative stiffness and damping properties of sandwich panels with aluminium and aramid cores within frequency sweeps ranging from 1 to 100 Hz. The analysis was also conducted with a temperature sweep analysis (varying the temperature within the temperature range of 0°–200°C) and it was demonstrated that the damping behaviour of the sandwich panel was dependent on the applied static load and core type. It should be noted that the sandwich structure with aluminium core was post-cured at a higher temperature (90°C) compared to the composite panels with the aramid core (65°C). The effect of this difference in post-cure schedule was demonstrated by the variation in the glass transition

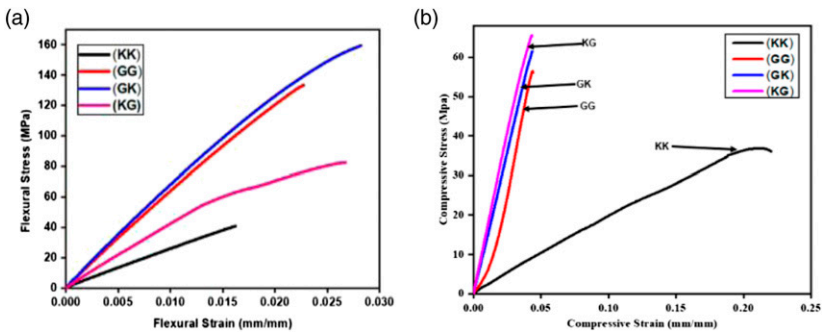

Figure 3. Stress-strain curves of composites sandwich structures with different face sheets: (a) flexural; (b) compressive. (KK – kenaf/kenaf, GG – glass/glass, GK – glass/kenaf, KG – kenaf/glass).[65]

Table 3. Summary of critical literature on compressive and flexural performance of composite sandwich structures.

Ref	Face sheet	Core	Resin	Variable	Dimension (mm)	Compressive		Flexural	
						Strength	E	Strength	E
[19]	GFRP	PET	Polyester	Core thickness	1200 × 400 × (40,60,80)	N/A	N/A	>187.6% (80 mm)	>53.6% (80 mm)
		GFRP web		Face thickness	(3, 3.75, 4.5)			>41.6% (4.5 mm)	>24.9% (4.5 mm)
[59]	GFRP	Polyurethane foam	Polyester	Core type	300 × 340 × 50	N/A	N/A		N/A
		Galvanized steel tooth nails		Core density					
				35 kg/m^3				>168%	
				80 kg/m^3				>211%	
				150 kg/m^3				>258%	
[66]	GFRP	Urethane	Polyester	Web thickness	200 × 200 × (2.4, 4.8, 7.2)	>2377.3%$^{\Delta}$ (7.2 mm)	>6416.4%[b] (7.2 mm)	N/A	N/A
				Web spacing	(50, 75, 100)	>72.8%[b] (75 mm)	>1700.5%[b] (7.2 mm)		
				Core density	(40, 60, 80)[a]	>26.7%[b] (80)	>14.7%[b] (80)		
[18]	GFRP	Wood	Epoxy	Core type	1400 × 80 × 120	N/A	N/A		
		GFRP web		Core design					
				1 × web				>138.5%[b]	>53.36%[b]
				2 × web				>141.97%[b]	>46.55%[b]
				3 × web				>147.6%[b]	>37.88%[b]
				4 × web				>153.1%[b]	>47.99%[b]

(continued)

Table 3. (continued)

Ref	Face sheet	Core	Resin	Variable	Dimension (mm)	Compressive		Flexural	
						Strength	E	Strength	E
[67]	GFRP	Wood-base core (control MDF honeycomb)	Polyester	Core type	200 × 75 × 25	N/A	N/A	>11.76%[b]	>14.11%[b]
				MDF + wheat straw				>185.4%[b]	>87.1%[b]
				Plywood				>39.83%[b]	>43.53%[b]
				Solid MDF					
[34]	GFRP	Paper honeycomb	Epoxy	Core type	130 × 50 × 15.5	>64.17% [Δ]	>85.87% [Δ]	N/A	N/A
[39]	GFRP	Poly urethane foam	Polyurethane	Core design	254 × 74.93 × 54.61	>214.8%	>1229.5%	>252%	>319%
				Trapezoid		>57.1%	>393.2%	>5%	>185.3
				Web					
[35]	GFRP	Nomex honeycomb (NHK)	Epoxy	Core type	200 ×15.5 × 40	N/A	N/A	Flatwise	Flatwise
								>30%	>30%
		Kraft honeycomb (KH)		Span	62 × 15.5 × 25				
					200 ×15.5 × 40			>30%	>30%
					62 × 15.5 × 25			Edgewise	Edgewise
								>25%	>30%
								>20%	>20%
[68]	CFRP	Al honeycomb	Epoxy	Face sheet design	300 × 30 20	N/A	N/A		
								N/A	N/A
				UD0/90				>4.33%	>6.22%
				TW0/UD0				<57.1%	>12.54%
				TW0/UD/90					
[69]	CFRP	Polyurethane foam	Epoxy	Loading rates	255 × 25.4 × 19	No change	N/A	N/A	N/A
				Crack location	255 × 25.4 × 39	>120%			

(continued)

Table 3. (continued)

Ref	Face sheet	Core	Resin	Variable	Dimension (mm)	Compressive		Flexural	
						Strength	E	Strength	E
[63]	CFRP	Al honeycomb	Epoxy	Face sheet design	125 × 46 × 18	N/A	N/A		
				DSH				1433.2 N	N/A
				PSH				1484.7 N	>287.3%
				USH				1605.5 N	>115.4%
[70]	CFRP	M-shaped lattice core	Epoxy	Core design	90 × 90 × 30	Core effect >18.7%[b]	N/A	Core effect >8.3%[b]	N/A
	Nano-SiO_2			Reinforcement		SiO_2 effect >18.8%[b]		SiO_2 effect >16.1%[b]	

[a]Density ρ (Kg/m^3).
[b]value for one sample type/configuration, E_{Abs} energy absorbed, > increase in performance, < decrease in performance.

temperature T_g of the epoxy used as matrix for the face sheets. As can be seen from Figure 4, the glass transition temperature (denoted by the peak in the loss modulus, E″) was higher (154°C) for the sandwich with aluminium core than that with the aramid core, which was at 119°C. This significant difference in values was in good agreement with the data measured for epoxy laminates with different thermal treatment. Additionally, it can be observed that the peak in the loss modulus (one in the sandwich with aluminium core and the first in the aramid-core specimen) was clearly due to the transition of the epoxy material used in the face sheet fabrication. The second peak was attributed to the phenolic resin used in the coating of the aramid core. Therefore, in this study, the use of DMA techniques provided sufficient information on the viscoelastic properties of the sandwich materials that could be used for optimization of the designs.

Mechanical impact

Over the years, researchers are in agreement that impact can be broadly categorized into two main groups: low-velocity and high-velocity. However, there still exists a lack of consensus on their definitions and what constitutes the transition from one to another. Some researchers have argued that low-velocity impact could be primarily viewed as quasi-static in nature.[74] The dynamic response of the specimen under this arrangement is such the contact duration is long enough for the entire respond thereby absorbing more energy. In terms of speed of the projectiles, most researchers consider the velocity range of low-velocity impact velocities below 100 m/s.[27,36,75] Researchers also group impacts according to the test techniques the loads generated by instrumented falling weight impact testing (Charpy, IZOD, drop weights etc.) are considered low velocity impact. On the other hand, high velocity impact is dominated by a fast stress (speed above 100 m/s) wave propagation through the material in which the structure does not have sufficient time to respond. Thus, boundary conditions effects do not play a major role as the impact event is over before the stress wave reaches the edge of the structure.[74] Additionally, a major difference between low-velocity and high velocity the nature of the damage experienced by the structure. Thus, low velocity is characterized by delamination and matrix cracking while in high velocity penetration-induced fibre breakage is most critical.[76]

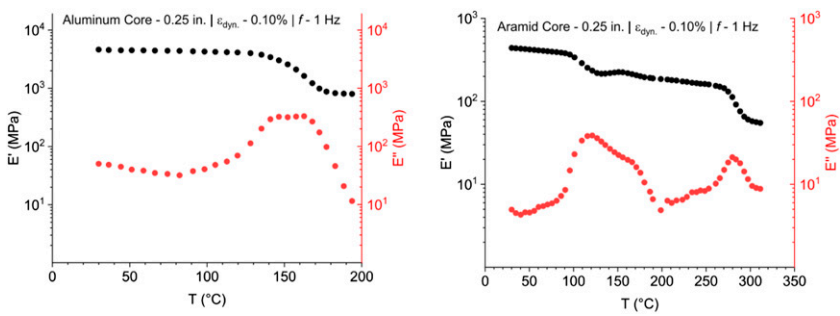

Figure 4. DMA temperature-sweep analysis for sandwich panels with two core types.[73]

Low-velocity impact. Under low-velocity impact, FRPSSs exhibit two-peak loading regimes attributed to the response of the FRP face sheets (top and bottom). A damage-initiation stage consists of local indentation of the face sheets with matrix cracking, followed by a penetration of the top face sheet as the damage evolves. Thereafter, as crushing and shearing of the core progresses, debonding between the core and the bottom face sheet occurs, after which excessive compression of the back sheet can lead to the eventual damage of the sample under repeated loading up to the material strength. Several researchers examined the response of FRP sandwich panels under such low-velocity impact loads.[20,77–80] Low-velocity drop weight tests were performed on the sandwich panels with carbon-fibre face sheets and cores manufactured from linear PVC, crosslinked PVC and PEI foams bounded together.[28] The test demonstrated that the peak load associated with the fracture of the rear skin was higher by nearly three times than that of the top skin. Specifically, the research established that placing the high-density core against the top face sheet can lead to improved impact resistance thanks to the core of the distal surface.

Chen et al. used the drop-weight technique to investigate the perforation of a sandwich panel with CFRP/epoxy face sheets and Nomex honeycomb core.[81] An impactor with a diameter of 12.5 mm at a speed of 2.23 m/s corresponding to initial energy of 22.25 J was used for this analysis. The results obtained were used to validate the quasi-static and dynamic properties of the panels in a numerical model. It was found that the damage characteristics were similar to the available data in the literature for fibre fracture/rupture, matrix crushing/cracking, and delamination as well as the core crushing and debonding. Modifications of the material properties of sandwich panels were made in some studies to mitigate damage in the plates. Ramakrishnan demonstrated that the inclusion of nanoparticles in the resin prevented the damage localization in the impact zone and ensured its spread across the structure.[24] Similarly, the inclusion of a layer of polyurea and polyurethane (PUR) between the face sheets and the core of sandwich structures as shown in Figure 5 demonstrated to improve the impact resistance significantly.[82] The work revealed

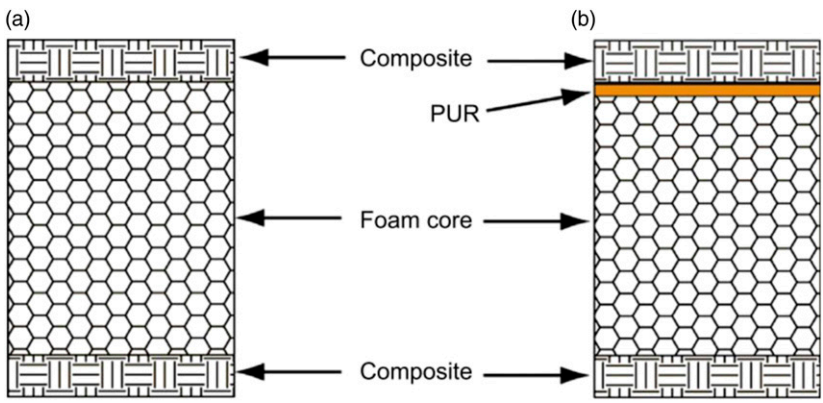

Figure 5. Modified sandwich structure: (a) conventional design. (b) modified design with PUR layer.[82]

that for a FRPSS specimen subjected to an impact energy of 67 J, the inclusion of the 1 mm- and 2 mm-thick PUR layer reduced the depth of indentation by 30% and 60%, respectively. The enhanced impact resistance was consistent, irrespective of the manufacturing process (vacuum infusion or hand-layup).

It is also common to use quasi-static indentation (QSI) analysis to identify the failure mechanisms in a low-velocity impact and the sequence of interactions between the constituents of the sandwich structure during such damage.[83–89] Owing to the similarities in the damage modes, several studies showed that the quasi-static indentation (QSI) method could give indications of the damage mods in LVI for composites.[84,90] Zniker et al.[61] used this method to compare the energy absorption capability of GFRP laminates and PVC-foam sandwich structures under repeated impacts and reduced energies using a modified Charpy test and QSI experiments. Their results revealed that while the indentation energy for the laminates with varying thicknesses was identical, the presence of the foam core significantly improved the damping properties of the sandwich structures. Furthermore, the damaged area of sandwich structures was larger than that in the laminates and predominantly in the form of delamination. Similar studies demonstrated that failure modes of sandwich structures due to QSI were similar to those by QSI, namely, core buckling, core crushing, delamination in face sheets, debonding between the core and face sheets as well as matric cracking and fibre breakage in the face sheets.[91–94] A typical force-displacement curve reflecting the initiation and evolution of damage in a sandwich panel under QSI is depicted in Figure 6.

High-velocity impact. FRPSS are also employed in applications that require resistance to blast/high-velocity loading regimes thanks to their considerable energy-dissipation capabilities. Unlike low-velocity loading conditions, panels subjected to ballistic impacts are controlled by stress-wave propagation and are independent of boundary conditions.[95] A typical high-velocity setup is depicted in Figure 7. The core of the structure is beneficial for this application since it allows the structure to undergo large plastic deformation at relatively constant stress, thereby, absorbing a large amount of kinetic energy before fracture. Generally, the study and use of sandwich structures as energy absorbers have increased in recent years.[96–101] Ivanez et al.[102] examined the effect of a cork core on the energy absorption properties of FRPSS under high-velocity impact loading, comparing it to corresponding laminates. It was observed that the ballistic limits (per areal density) for intact panels (sandwich and laminates) were similar, while already damaged ones exhibited a variation of about 36%. Thus, the study revealed that under high-velocity loading sandwich panels with cork cores displayed no significant improvement in energy absorption for intact samples except for panels that were previously damaged.

The effects of a high-velocity projectile on the front and back face sheets of the sandwich panels provide useful information for the optimization of the structure for the ballistic application. The assessment of the energy-absorption capabilities of CFRP face sheets with an aluminium-honeycomb core sandwich panel revealed that more than 70% of the kinetic energy was absorbed by the front face sheet.[21]

Usta et al.[104] studied the performance of CFRP/epoxy sandwich panels subjected to an impact with a 10 mm impactor at 100 m/s. A response of a doubly curved panel was

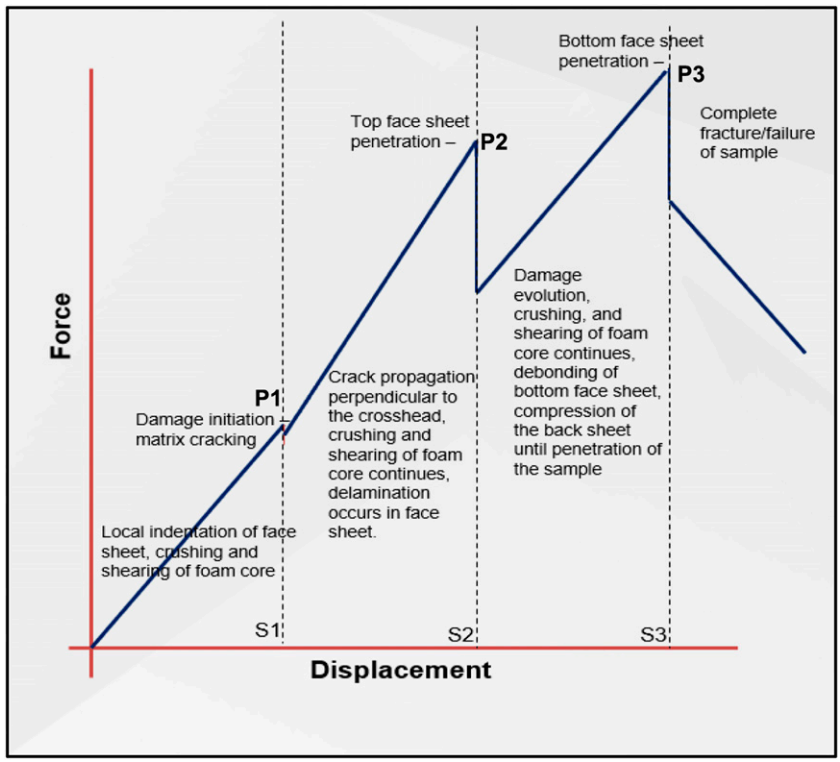

Figure 6. Damage evolution of typical sandwich panel under the low-velocity impact (QSI) adapted from.[83]

compared to that of a flat one while different performances of two types of cores (polyurethane foam and 3D printed PLA plastic cellular auxetic honeycombs) were studied. It was revealed that the spherical sandwich panels have lower impact resistance compared to the flat panels for both core designs. Further assessment of the core designs revealed that, the re-entrant configuration had a better specific energy absorption (SEA) capacity than the foam core and thus a better impact resistance under large deformations. The perforations of the entrant and foam core doubly curved specimens is shown in Figures 8 and 9. Details of selected studies on high-velocity impact performance and main corresponding outcomes are presented in Table 4.

Numerical investigations

Multi-scale simulations

For the meso and macro scales, various researchers developed models to accurately predict and characterize the damage mechanism of FRPSS. However, the precise analysis

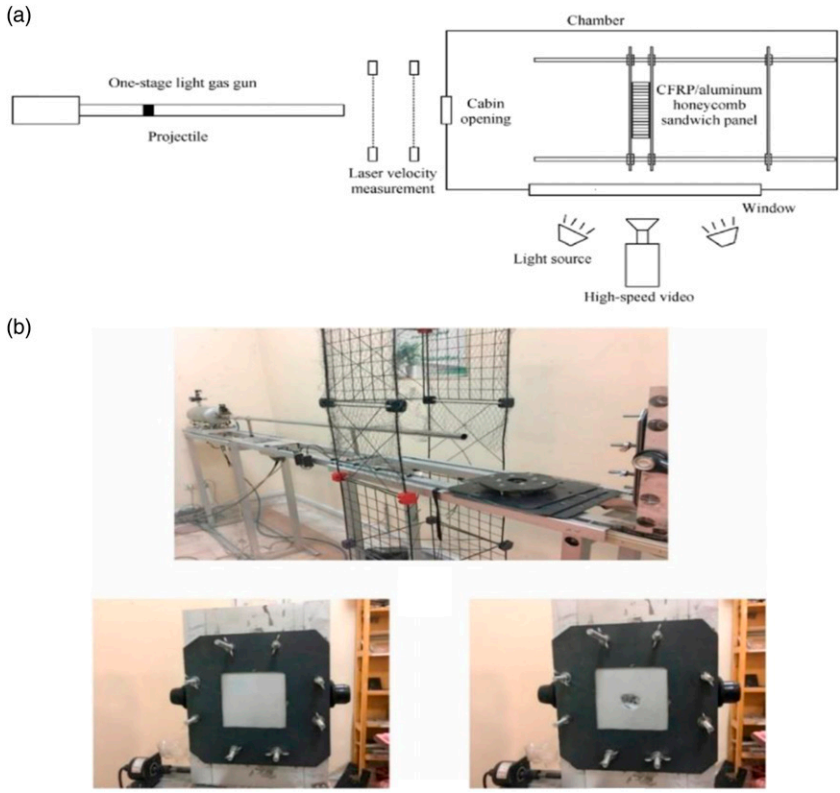

Figure 7. High-velocity impact system: (a) one-stage light-gun schematic setup,[21] (b) experimental setup with sample before and after impact.[103]

of the constituents has been a challenge, as most commercial FEA packages require material properties to model the face sheets and cores. This led to the development of subroutines that generate better numerical models for the constituent materials.[62,111–117] This section focuses on principles and theories adopted in the development of numerical models related to flexural, single-cantilever, compressive, and impact tests of FRPSS.

Quasi-static numerical models. Several studies were conducted on the development of numerical models that can be used in the validation of the macro- and meso-damage of FRPSS. These studies have investigated the fracture characteristics,[118–120] flexural properties,[60,121,122] and compression behavior [123] of such structures with two and three-dimensional models. Farshidi et al.[16] developed a 2D FEA model of a disbonded honeycomb-core sandwich structure using the crack surface displacement extrapolation method to investigate the energy release rate and mode-mixity of the panels. The model consisted of CFRP face sheets and Nomex honeycomb core and was benchmarked against the experimental results and closed-form semi-analytical models of the same

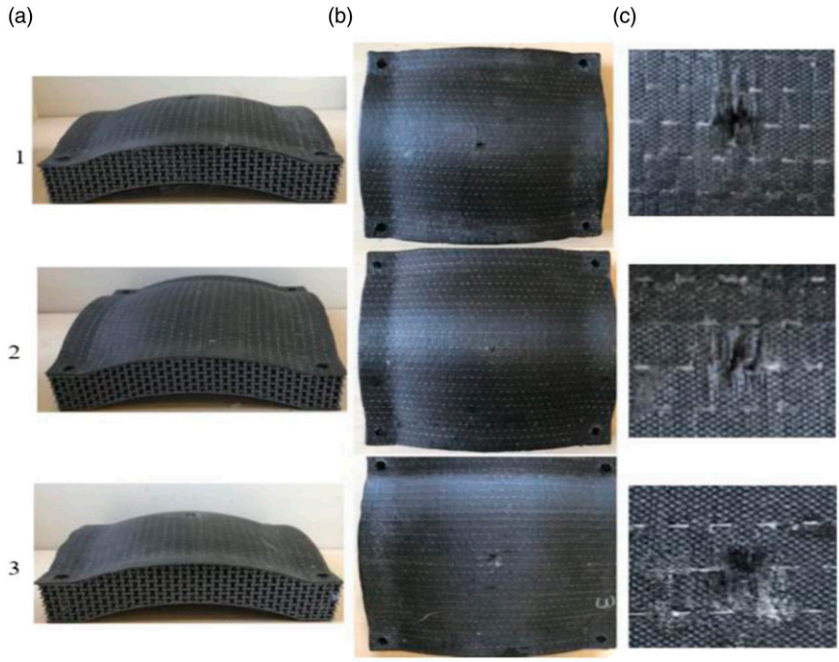

Figure 8. Damage characterization of a doubly curved sandwich panel with entrant core: (a) cross-section; (b) top view; (c) top view of impact zone.[104]

configuration. The results showed that the energy release rate and the mode-mixity were constant, which also validated the mode-I-dominated damage in the setup. The simulation revealed that the crack length and the thickness of the bonded area had a significant effect on the energy release rate while the Poisson's ratio, cell size, and thickness had a more significant effect on the mode-mixity value. In a similar work, Zhao et al.[122] utilized an FEA model with multi-layered 4-node general-purpose shell elements for the sandwich structure to accurately predict crack propagation in glue seams and failure of novel pultruded GFRP facesheets with foam cores under flexural loading, which was validated by experimental data. The damage initiation in the GFRP facesheets was assessed based on the Hashin damage criteria and the cracking of the glue seams was predicted by defining the fail stresses obtained from the material properties of the specimen. According to this study, the simplified model was limited in capturing delamination and shear crack failures of these configurations of GFRP sandwich structures used in wind turbine blades.

In another study,[62] a user-defined subroutine based on the Hashin's 3D failure criteria was utilized to simulate the crushing behaviour of the foam-filled core sandwich structure with E-glass face sheets with varying slenderness ratios. The results showed that the first and second-order buckling modes played a significant role in the crushing behaviour of the sandwich columns with high slenderness. The failure progression of the sandwich

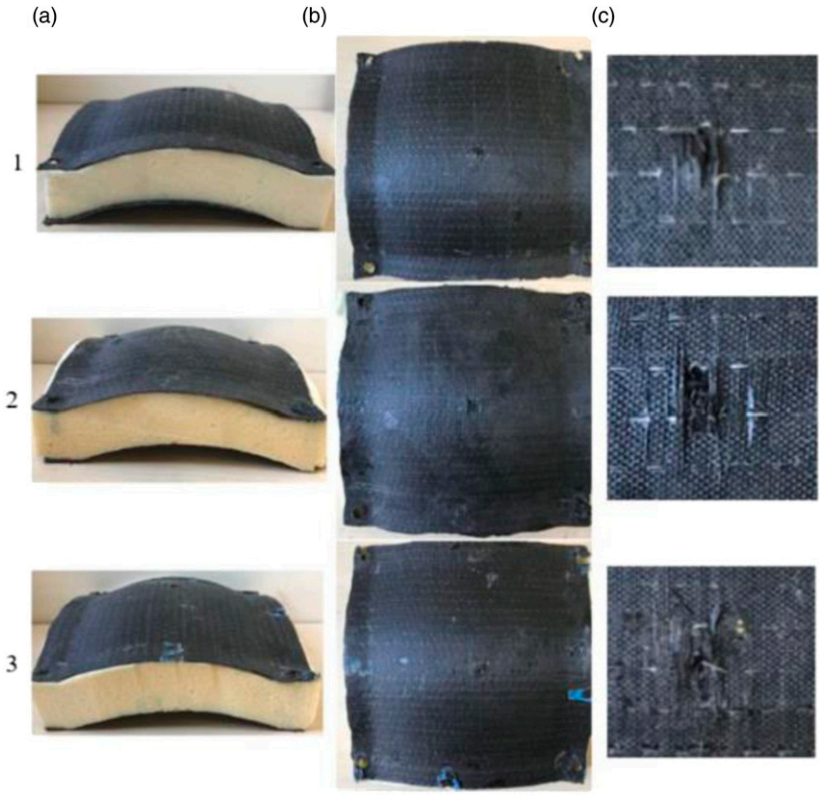

Figure 9. Damage characterization of a doubly curved sandwich panel with foam core: (a) cross-section; (b) top view; (c) top view of impact zone.[104]

column under edgewise compression loads from initiation to total fracture is described in Figure 10.

A 3-dimensional numerical model based on continuum damage mechanics (CDM) with a Hashim failure criterion was successfully employed in[19] to understand the failure modes and responses of sandwich structures with GFRP facesheets and a PET foam core subjected to 4-point bending. The model adequately captured the failure modes, load-displacement behaviour, and peak loads of the panel. So, it was used to conduct a parametric study, varying parameters of the lattice web (the arrangement of FRP along the through-thickness direction of the FRPSS at specified intervals) and spacing of the core. The results revealed that the peak load and flexural stiffness increased substantially with increasing lattice web thickness, while the lattice spacing had little effect on the level of stiffness and load-carrying capacity. It is worth noting that the Hashin initiation criterion, determining the onset and propagation of damage, is widely used in the literature to predict the tensile and compressive failure of the fibre-reinforcement and the matrix in most numerical simulations reveiwed.[19,124,125]

Table 4. Summary of selected literature on penetration performance of composite sandwich structures.

Ref	Face sheet	Core	Resin	Type of impact	Indenter/ projectile	Dimension (mm)	Experiment	Variable	Main findings
[92]	GFRP	PVC foam Balsa wood Al honeycomb	Vinyl ester	Low velocity (9 J–30 J)	Spherical 12.7 cm[d] 4.76 kg[w]	27.9 × 27.9 × 2.82	Drop weight	•Core type •Impact energy	•Impact energy and type of core significantly affects failure patterns
[89]	CFRP	Foam/CFRP bar pins	Epoxy	Quasi-static (0.5 mm/min)	Spherical 10 mm[d]	60 × 60 × 7.5	QSI	•Configuration •Inclination angle •Pinning density	•Effect of inclination angle negligible •Inserted pins stiffen the core significantly •The position of pins in relation to the loading point affects indentation properties
[20]	CFRP	PVC	Epoxy	Low velocity (1 J–9 J)	Spherical 16 mm[d] 4.76 kg[w]	150 × 100 × 6.35	Drop weight	•Temperature •Impact energy •Face sheet (t)	•Impact behaviour is affected by temperature significantly •Extreme low temp reduces impact resistance and causes complex damage mechanisms
[24]	Kevlar	PMC	Epoxy	Low velocity (8 J, 12 J and 16 J)	Hemispherical 16 mm[d] 1.8 kg[w]	200 × 200 × 20	Drop weight	•Reinforcements in matrix •Impact energy	•Reinforcements improved perforation resistance •Non-localized damage in foam core
[105]	CFRP	Polyurethane foam	Epoxy	Low velocity (3 J–6 J)	Hemispherical 12.7 mm[d] 2.64 kg[w]	150 × 100 × 6	Drop weight	•Stich row spacing •Impact energy	•Stitches reduce damage area •Stich thread acts as crack initiation and cracks arrestor in delamination •The delamination area increases with increased energy
[77]	CFRP	Expended Cork	Epoxy	Low velocity (10 J)	Hemispherical 12.7 mmd	76.2 × 76.2 × 9.7	Drop weight	•Core design	•Cork core has a higher impact resistance than PMI.
[82]	GFRP	Foam core PUR	Epoxy	Quasi-static (5 mm/min)	Hemispherical 74 mm[d]	152 × 152 × (24.3, 25)	QSI	•Core design •Fabrication method	•PUR increases penetration resistance •Change in thickness of PUR insignificant to impact resistance
				Low velocity (67 J)	Hemispherical 20 mm[d] 3.4 kg[w]		Drop weight		•PUR increases impact resistance •The fabrication method affects the depth of indentation
[23]	CFRP	Polyurethane core	Vinyl ester	Low velocity (4.45 J–23.7 J)	Hemispherical (Cylindrical) 20 mmd/40 mm[d] (40 mm[d]) 6.16 kg[w] (6.27 kg[w])	245 × 245 × (7, 18)	Drop weight	•Core thickness •Impactor size •Impact energy	•Shorter impact response time for the larger core •The degree of sharpness of the impactor affects dynamic response •Core with ATH dissipates a considerable amount of impact
[78]	GFRP	Alumina tri-hydrate (ATH) particles	Epoxy	Low velocity (20 J–50 J)		51 × 51 × 25.4	Drop weight	•Core design •Impact energy	

(continued)

Table 4. (continued)

Ref	Face sheet	Core	Resin	Type of impact	Indenter/ projectile	Dimension (mm)	Experiment	Variable	Main findings
[106]	CFRP	Aramid honeycomb	Epoxy	Low velocity (3 J, 6 J and 10 J)	Spherical 16 mm^{d} 5.607 kg^{w}	100 × 150 × (8, 16)	Drop weight	•Core thickness •Impact energy	•The deformation pattern is local for the thicker core and global for the thinner core •Dent, delamination, and absorbed energy increases with increased energy
[22]	CFRP	Nomex honeycomb	Epoxy	Low velocity (3 J, 5 J, 7 J and 10 J)	Hemispherical 20 mm^{d} 3.620 kg^{w}	12 × 120 × 12.4	Drop weight	•Impact angles •Impact energy	•The damaged area decreases with increasing angle •Absorbed energy decreases with an increase in angle
[28]	CFRP	Linear PVC Cross-link PVC PEI	Epoxy	Low velocity (40.8 J)	Hemispherical	100 × 100 × 30.7	Drop weight	•Density of core •Thickness	•failure is predominately due to core shear •placing a higher-density core under the top face sheet increases perforation resistance
[21]	CFRP	Aluminium honeycomb	Epoxy	High velocity (260.5 m/s, 276.4 m/s, 281.3 m/s and 290.6 m/s)	Al projectile 15.3 mm^{d} 7.47 g^{w}	120 × 120 × 3	Light weight gas gun	•Velocity •Core type	•Over 70% of kinetic energy is absorbed by the face sheet and honeycomb core
[107,108]	GFRP/Al Alloy	Polyurethane foam	Epoxy	High velocity (400 m/s)	Flat-ended cylindrical 5 mm^{d} (4.52 mm^{d}) 12.2 g^{w} (14.6 g^{w})	150 × 150 × 7.96	Gas gun	•Layup sequence •Core density •Projectile •Impact energy	•increase in petal shape of the impacted bottom face due to impact energy •Core density has the least effect on energy absorption •Different patterns of crack propagation in front and back face sheets
[104]	CFRP	Polyurethane 3D-PLA honeycomb	Epoxy	High velocity (100 m/s)	Steel projectile 10 mm^{d}	200 × 200 × 30	Single-stage air gas gun	•Sample design •Core type	•Flat panels exhibit higher impact resistance than curved panels •Re-entrant lattice core has higher SEA than foam core
[109]	CFRP	Nomex honeycomb	Epoxy	High velocity (797 m/s, 818 m/s and 950 m/s)	Live projectiles (5.56 mm, 6.5 mm, 7.63 mm)	500 × 500 × 12	Live firearms	•Projectile calibre •Target angle	•Oblique impacts have extensive and elliptical damage •Projection calibre has limited effects on damage mechanism
[110]	GFRP	Plywood	Epoxy nylon 6	High velocity (220 m/s)	Conical 10 mm^{d} 9.12 g^{w}	120 × 120 × 13.4	Gas gun	•Face sheets design •Matrix type	•carbon nanotubes improve impact resistance •rear face sheet damage area reduces with reinforcements •GFRP/epoxy has more energy absorption than GFRP/nylon face sheets

w = weight, d = diameter.

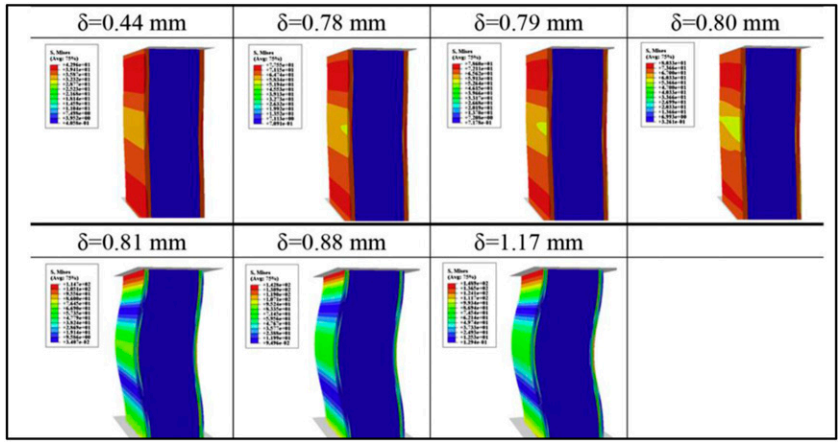

Figure 10. Failure progression of foam-filled sandwich column under edgewise compression loading.[62]

Dynamic numerical models. Various studies developed damage models for sandwich plates subjected to dynamic loads,[28,126] with the dynamic behaviour of foam sandwich panels subjected to low, high and ballistic impacts were simulated. Foo et al.[127] suggested a modified energy-balance model to predict the low-velocity impact response for sandwich composites subjected to the QSI loading regiment. The model incorporated the law of conservation of momentum to extend its accuracy beyond the elastic region of the materials as it accounted for damage initiation and propagation. The dynamic response and the progressive damage evolution of composite lattice sandwich panels were investigated numerically using the coupled-Eulerian-Lagrangian method.[128–130] The study identified fibre fracture as the most significant damage mode and the need to optimize the structures in naval applications. Furthermore, the model accurately captured the phenomena of matrix cracking and delamination. Chen et al. developed a predictive FEA model that could capture the damage mechanism of composite sandwich structures fabricated from CFRP facesheets and Nomex honeycomb core.[81] The model utilized the CDM approach to characterize the inter and intra-laminar damage as well as the effects of adhesive and strain rate on the structure, which was modelled with ABAQUS/Explicit software.[131] Interestingly, in the constitutive model developed by Gao et al.,[21] the Hashin failure criterion was used for the laminates, while the Johnson-Cook failure model was employed for the aluminium honeycomb cores. The facesheets and the core were assigned appropriate material properties while the projectile had the material properties of aluminium alloy with 8-node reduced integral solid elements. Universal contact and encastre boundary conditions were used for the model. The simulation adequately described the damage mechanism of the sandwich plate from (Figure 11) at the onset (t = 15 μs) to the perforation (165 μs). It is worth noting that a variety of models available in commercial FEA packages can be used to characterize damage in sandwich structures subjected to dynamic loads; however, it is common to find that, for some simulations, researchers

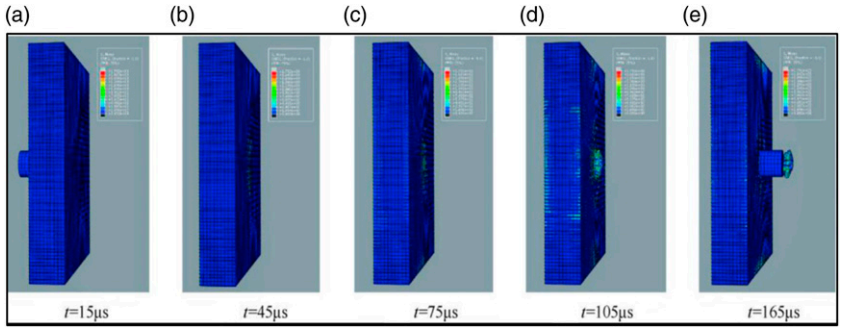

Figure 11. Timestamp of stress distribution of projectile striking composite sandwich structures.[21]

incorporated user-defined material subroutines, developed in a programming language such as FORTRAN or. This situation comes with added computational cost and inherent complexity; therefore, simplified models are commonly employed where applicability permits.

Environmental degradation

FRPSS are rather versatile in application, especially in harsh environments. They are used in a wide range of marine structures, where environmental degradation could lead to the onset of corrosion. These structures range from boats, yachts, and submarines as well to tidal turbines. It is well known that composite materials experience a significant water uptake[132,133] as well as swelling due to the variance in the water absorption nature of fibres and matrix.[134,135] This situation inevitably affects the constituent's interface and thereby leading to premature delamination of the composite.[136] Researchers have assessed the effects of salinity on the degradation of several types of FRPs under seawater conditions, showing that the moisture intake acted as a plasticizer of the polymer network in the structures.[137] With chemical treatment, natural FRP composites subjected to salt-fog degradation were found to exhibit better retention of their flexural properties. The study elucidated the effects of water absorption on the anisotropic mechanical response of epoxy resin reinforced with E-glass fibres. Samples were immersed in distilled water at 50°C for different durations until saturation, after which the samples were redried and also tested to determine the recoverability of the original mechanical properties.[138] The obtained results showed that the maximum moisture uptake was 0.71%, with saturation after 1200 h of exposure. Thereafter, tensile and three-point bending tests results indicated that the tensile strength, shear strength, and elastic modulus reduced by 40.5%, 17.6%, and 55.6%, respectively. The redried samples, however, demonstrated partial recovery of the mechanical properties of the samples. Moisture absorption can be measured in line with[139,140] employing the following equation:

$$M_g = \left(\frac{M_t - M_o}{M_o}\right)^2 \times 100\% \quad (1)$$

where M_g is the percentage of moisture gained, and M_t and M_o are the weights of the wet and dry samples at a specific time, respectively. Moreover, the water diffusion coefficient D could be obtained from the gravimetric calculations:

$$D = \pi\left(\frac{h}{4M_\infty}\right)^2\left(\frac{M_t - M_o}{\sqrt{t_2} - \sqrt{t_1}}\right)^2 \quad (2)$$

where M_∞ is the wate uptake at saturation, h is the thickness of the specimen, $\frac{M_t - M_o}{\sqrt{t_2} - \sqrt{t_1}}$ is the slope of the curve in the time range $(t_2 - t_1)$.

Hailin et al.[141] investigated the effects of seawater aging on the static/dynamic mechanical properties of CFRP laminates. The samples were degraded under varying temperatures (30°C–100°C and 27°C–34°C) and salinity conditions (0%, 3.5%, and 5%) for 7 months, after which tensile and DMA tests were performed. It was observed that the moisture absorption was *fickian* in nature, and the dynamic equilibrium was achieved after 90 days. Thereafter, the absorption was slower and less affected by temperature (*non-fickian*) until the equilibrium after 7 months was reached. The tensile strength of the samples was reduced by a maximum of 11.5% from 923.60 MPa to 817.83 MPa, revealing an exponential degradation relationship between the tensile strength and the aging time. Furthermore, the tensile strength was reduced by 16% due to temperature variation over the period, while its maximum reduction due to NaCl concentration was found to be 8.2%. Damping (tan δ) was observed to increase exponentially, while the glass transition temperature (Tg) reduced with prolonged seawater aging, a phenomenon attributed to the fibre/matrix interface of the laminates. For FRPSS, several studies were conducted to investigate the mechanical properties of the core which showed promise for its application in a marine environment. For instance, synthetic foams made from the fusion of hollow particles in a matrix exhibited higher specific properties compared to polymeric ones.[26–28,142,143] Also, the compressive properties of synthetic foams subjected to hygrothermal conditions at various temperatures were studied by Gupta et al. In this work, synthetic foam cores were subjected to deionized and seawater conditions, and their flexural properties were investigated. It was observed that the deterioration of the Youngs modulus in samples immersed in deionized water was higher than the ones exposed to seawater with salinity of 35% and 30% respectively. This substantial reduction in flexural properties was attributed to the degradation of matrix-particle interfaces due to moisture ingress or the degradation of the particles themselves.[144]

Challenges and future direction

The last two decades have witnessed scientific advancement in the field of mechanical performance of composite sandwich structures. However, it must be noted that this field is still evolving as novel FRP sandwich materials are increasingly emerging. While many studies were conducted on the characterization of the mechanical behaviour of FRP

sandwich panels using experimental and numerical techniques under quasi-static and impact loading regimes, their viscoelastic properties are still studied insufficiently. Some research was performed for the viscoelastic performance of composite sandwich specimens using the DMA methods and subsequently developing corresponding numerical models for validation. Furthermore, the reviewed articles indicated that substantial work was done on the environmental degradation of composite sandwich panels but the effects of these factors (particularly seawater degradation) on the viscoelastic parameters are still unclear; hence, it is a vital area to explore for understanding the nature of damage of FRPSS. It is necessary, therefore, to aggregate the data in these areas to further unravel the mechanical performance of the panels, especially as the scope of the application of composite sandwich structures for maritime use are ever-increasing. This will allow the optimization of sandwich panels for such applications.

Concluding remarks

This review investigated the latest advances in the characterization of the mechanical properties of FRPSS, analyzing and fabrication methods. Several experimental results from the literature highlighted the elastic-plastic and impact behaviour of composite sandwich structures and proved that the performance of the specific sandwich panels is influenced by several factors. It also provided insight into the environmental effects of moisture absorption (seawater) on mechanical performance. Thus, an in-depth understanding of the mechanical performance of the structures is important for any researcher to ensure optimal design. Several parameters used to develop numerical models were reviewed and it was established that although the Hashin failure criterion is popular, other researchers adopted case-study-specific criteria to characterize the damage in their respective models. The review was able to identify the viscoelastic properties of sandwich panels, especially after environmental degradation as a viable area of research. This should be guided by numerical simulations validated with experimental data.

Generally, this review provided a synopsis of the work done on elucidating the mechanical properties of sandwich structures under quasi-static and dynamic loading using experimental and numerical methods. Additionally, it aims to serve as a basis for investigating the viscoelastic properties under varying environmental conditions of future sandwich materials.

Acknowledgments

The authors acknowledge the support of Loughborough University and the Nigerian Air Force Research and Development Centre.

Declaration of conflicting interests

The author(s) declared no potential conflicts of interest with respect to the research, authorship, and/or publication of this article.

Funding

The author(s) disclosed receipt of the following financial support for the research, authorship, and/or publication of this article: This work was supported by the Nigerian Air Force under grant OPS/1282DTG27145AJUL21.

ORCID iDs

Norman Osa-uwagboe https://orcid.org/0000-0002-6560-445X
Emrah Demirci https://orcid.org/0000-0002-9052-1488

References

1. Altin Karataş M and Gökkaya H. A review on machinability of carbon fibre reinforced polymer (CFRP) and glass fibre reinforced polymer (GFRP) composite materials. *Def Technol* 2018; 14: 318–326.
2. Stickel JM and Nagarajan M. Glass fiber-reinforced composites: from formulation to application. *International Journal of Applied Glass Science* 2012; 3: 122–136.
3. Daniel IM and Ishai O. *Engineering Mechanics of Composite Materials*. Oxford, UK: Oxford University Press, 2006.
4. Langdon GS, von Klemperer CJ, Rowland BK, et al. The response of sandwich structures with composite face sheets and polymer foam cores to air-blast loading: preliminary experiments. *Engineering Structures* 2012; 36: 104–112.
5. Siriruk A, Jack Weitsman Y and Penumadu D. Polymeric foams and sandwich composites: material properties, environmental effects, and shear-lag modeling. *Composites Science and Technology* 2009; 69: 814–820.
6. Studzinski R, Pozorski Z and Garstecki A. Sensitivity analysis of sandwich beams and plates accounting for variable support conditions. *Bull Polish Acad Sci Tech Sci* 2013; 61: 201–210.
7. Prasad S and Carlsson LA. Debonding and crack kinking in foam core sandwich beams-II. Experimental investigation. *Engineering Fracture Mechanics* 1994; 47: 825–841.
8. Gosowski B and Gosowski M. Exact solution of bending problem for continuous sandwich panels with profiled facings. *Journal of Constructional Steel Research* 2014; 101: 53–60.
9. Osei-Antwi M, de Castro J, Vassilopoulos AP, et al. Shear mechanical characterization of balsa wood as core material of composite sandwich panels. *Construction and Building Materials* 2013; 41: 231–238.
10. Ashby F. Overview no. 80. *Acta Metallurgica* 1989; 37: 1273–1293.
11. Hasanalizade F and Dabiryan H. Theoretical modeling of low-velocity impact behavior of sandwich-structured composites reinforced with weft-knitted spacer fabric. *J Ind Text* 2022; 52: 1–21.
12. Delavari K and Dabiryan H. Effect of Z-fiber orientation on the bending behavior of sandwich-structured composite: numerical and experimental study. *Composite Structures* 2021; 256: 113140.
13. Clyne T and Hull D. General Introduction. In: *An Introduction to Composite Materials*. Cambridge, UK: Cambridge University Press, 2019, pp. 1–7.
14. Wang R-M, Zheng S-R and Zheng Y-P. Molding technology of sandwich structure composites. *Polymer Matrix Composites and Technology* 2011: 321–548.

15. Daniel IM, Gdoutos EE and Rajapakse YDS. Major accomplishments in composite materials and sandwich structures: an anthology of ONR sponsored research. In: *Major Accomplishments in Composite Materials and Sandwich Structures: An Anthology of ONR Sponsored Research*. Dordrecht: Springer, 2009, pp. 1–818.
16. Farshidi A, Berggreen C and Schäuble R. Numerical fracture analysis and model validation for disbonded honeycomb core sandwich composites. *Composite Structures* 2019; 210: 231–238.
17. Abdulaziz AH, Hedaya M, Elsabbagh A, et al. Acoustic emission wave propagation in honeycomb sandwich panel structures. *Composite Structures* 2021; 277: 114580.
18. Shi H, Liu W, Fang H, et al. Flexural responses and pseudo-ductile performance of lattice-web reinforced GFRP-wood sandwich beams. *Composites Part B: Engineering* 2017; 108: 364–376.
19. Xie H, Shen C, Fang H, et al. Flexural property evaluation of web reinforced GFRP-PET foam sandwich panel: experimental study and numerical simulation. *Composites Part B: Engineering* 2022; 234: 109725.
20. Feng D and Aymerich F. Damage prediction in composite sandwich panels subjected to low-velocity impact. *Composites Part A: Applied Science and Manufacturing* 2013; 52: 12–22.
21. Gao G, Tangling E, Feng M, et al. Research on dynamic response characteristics of CFRP/Al HC SPs subjected to high-velocity impact. *Defence Technology* 2018; 14: 503–512.
22. Ivañez I, Moure MM, Garcia-Castillo SK, et al. The oblique impact response of composite sandwich plates. *Compos Struct* 2015; 133: 1127–1136.
23. He Y, Zhang X, Long S, et al. Dynamic mechanical behavior of foam-core composite sandwich structures subjected to low-velocity impact. *Archive of Applied Mechanics* 2016; 86: 1605–1619.
24. Ramakrishnan KR, Guérard S, Viot P, et al. Effect of block copolymer nano-reinforcements on the low velocity impact response of sandwich structures. *Composite Structures* 2014; 110: 174–182.
25. Carlsson LA and Kardomateas GA. *Structural and Failure Mechanics of Sandwich Composites*. Berlin, Germany: Springer, 2011, pp. 1–17. DOI: 10.1007/978-1-4020-3225-7_1.
26. Flores-Johnson EA, Li QM and Mines RAW. Degradation of elastic modulus of progressively crushable foams in uniaxial compression. *Journal of Cellular Plastics* 2008; 44: 415–434.
27. Zhou J, Hassan MZ, Guan Z, et al. The low velocity impact response of foam-based sandwich panels. *Composites Science and Technology* 2012; 72: 1781–1790.
28. Zhou J, Guan ZW and Cantwell WJ. The impact response of graded foam sandwich structures. *Composite Structures* 2013; 97: 370–377.
29. Kee Paik J, Thayamballi AK and Sung Kim G. The strength characteristics of aluminum honeycomb sandwich panels. *Thin-Walled Structures* 1999; 35: 205–231.
30. Heimbs S, Schmeer S, Middendorf P, et al. Strain rate effects in phenolic composites and phenolic-impregnated honeycomb structures. *Composites Science and Technology* 2007; 67: 2827–2837.
31. Foo CC, Seah LK and Chai GB. Low-velocity impact failure of aluminium honeycomb sandwich panels. *Composite Structures* 2008; 85: 20–28.

32. Gupta N, Ye R and Porfiri M. Comparison of tensile and compressive characteristics of vinyl ester/glass microballoon syntactic foams. *Composites Part B: Engineering* 2010; 41: 236–245.
33. Tao XF and Zhao YY. Compressive failure of Al alloy matrix syntactic foams manufactured by melt infiltration. *Materials Science and Engineering: A* 2012; 549: 228–232.
34. Kumar SJA and Ahmed KS. Compression behavior and energy absorption capacity of stiffened syntactic foam core sandwich composites. *Journal of Reinforced Plastics and Composites* 2013; 32: 1370–1379.
35. Kumar SJA and Ahmed KS. Flexural behavior of stiffened syntactic foam core sandwich composites. *Journal of Sandwich Structures & Materials* 2014; 16: 195–209.
36. Abrate S. Impact on laminated composite materials. *Applied Mechanics Reviews* 1991; 44: 155–190.
37. El-Hassan H, El-Maaddawy T, Al-Sallamin A, et al. Performance evaluation and micro-structural characterization of GFRP bars in seawater-contaminated concrete. *Construction and Building Materials* 2017; 147: 66–78.
38. Vanlandingham MR, Eduljee RF and Gillespie JW. Moisture diffusion in epoxy systems. *Journal of Applied Polymer Science* 1999; 71: 787–798.
39. Mohamed M, Anandan S, Huo Z, et al. Manufacturing and characterization of polyurethane based sandwich composite structures. *Composite Structures* 2015; 123: 169–179.
40. Davies P. Environmental degradation of composites for marine structures: new materials and new applications. *Philosophical Transactions of the Royal Society A: Mathematical, Physical and Engineering Sciences* 2016; 374: 20150272. DOI: 10.1098/rsta.2015.0272.
41. Ghabezi P and Harrison NM. Hygrothermal deterioration in carbon/epoxy and glass/epoxy composite laminates aged in marine-based environment (degradation mechanism, mechanical and physicochemical properties). *Journal of Materials Science* 2022; 57: 4239–4254.
42. Zhao Q, Zhang D, Zhao XL, et al. Modelling damage evolution of carbon fiber-reinforced epoxy polymer composites in seawater sea sand concrete environment. *Composites Science and Technology* 2021; 215: 108961. DOI: 10.1016/j.compscitech.2021.108961.
43. Khan MH, Elamin M, Li B, et al. X-ray micro-computed tomography analysis of impact damage morphology in composite sandwich structures due to cold temperature arctic condition. *Journal of Composite Materials* 2018; 52: 3509–3522.
44. Mathieson H and Fam A. High cycle fatigue under reversed bending of sandwich panels with GFRP skins and polyurethane foam core. *Composite Structures* 2014; 113: 31–39.
45. Triantafillou TC and Gibson LJ. Failure mode maps for foam core sandwich beams. *Materials Science and Engineering* 1987; 95: 37–53.
46. Shenhar Y, Frostig Y and Altus E. Stresses and failure patterns in the bending of sandwich beams with transversely flexible cores and laminated composite skins. *Composite Structures* 1996; 35: 143–152.
47. Thomsen OT and Frostig Y. Localized bending effects in sandwich panels: Photoelastic investigation versus high-order sandwich theory results. *Composite Structures* 1997; 37: 97–108.

48. Frostig Y and Shenhar Y. High-order bending of sandwich beams with a transversely flexible core and unsymmetrical laminated composite skins. *Science* 1995; 5: 405–414.
49. Mazaheri F and Hosseini-Toudeshky H. Experimental investigations of static and fatigue crack growth in sandwich structures with foam core and fibre-metal laminates face sheets. *AUT J Mech Eng* 2018; 2: 149–164.
50. Rizov V. Mixed-mode I/III fracture study of sandwich beams. *Cogent Engineering* 2015; 2: 993528. Epub ahead of print 2015. DOI: 10.1080/23311916.2014.993528.
51. Quispitupa A, Berggreen C and Carlsson LA. Face/core interface fracture characterization of mixed mode bending sandwich specimens. *Fatigue & Fracture of Engineering Materials & Structures* 2011; 34: 839–853.
52. Kabir K, Vodenitcharova T and Hoffman M. Response of aluminium foam-cored sandwich panels to bending load. *Composites Part B: Engineering* 2014; 64: 24–32.
53. Dhaliwal GS. Characteristics of CFRP/PU foam and GFRP/PU sandwich beams having initial debond between facesheet and core. *SN Appl Sci* 2021; 3: 1–11.
54. Newaz G, Dhaliwal GS, Phadatare A, et al. Effect of padding on flexural response of sandwich composites. *Journal of Sandwich Structures & Materials* 2021; 23: 1253–1271.
55. Zhu X, Xiong C, Yin J, et al. Bending experiment and mechanical properties analysis of composite sandwich laminated box beams. *Materials* 2019; 12: 2959. DOI: 10.3390/ma12182959.
56. Liu Q, Xu X, Ma J, et al. Lateral crushing and bending responses of CFRP square tube filled with aluminum honeycomb. *Composites Part B: Engineering* 2017; 118: 104–115.
57. Manalo AC, Aravinthan T and Karunasena W. Flexural behaviour of glue-laminated fibre composite sandwich beams. *Composite Structures* 2010; 92: 2703–2711.
58. Fotsing ER, Leclerc C, Sola M, et al. Mechanical properties of composite sandwich structures with core or face sheet discontinuities. *Composites Part B: Engineering* 2016; 88: 229–239.
59. Xie H, Wan L, Wang B, et al. An investigation on mechanical behavior of tooth-plate-glass-fiber hybrid sandwich beams. *Advances in Polymer Technology* 2020; 2020: 1–11. DOI: 10.1155/2020/6346471.
60. Sayahlatifi S, Rahimi GH and Bokaei A. The quasi-static behavior of hybrid corrugated composite/balsa core sandwich structures in four-point bending: Experimental study and numerical simulation. *Engineering Structures* 2020; 210: 110361.
61. Zniker H, Ouaki B, Bouzakraoui S, et al. Energy absorption and damage characterization of GFRP laminated and PVC-foam sandwich composites under repeated impacts with reduced energies and quasi-static indentation. *Case Studies in Construction Materials* 2022; 16: e00844.
62. Lei H, Yao K, Wen W, et al. Experimental and numerical investigation on the crushing behavior of sandwich composite under edgewise compression loading. *Composites Part B: Engineering* 2016; 94: 34–44.
63. Han Q, Qin H, Liu Z, et al. Experimental investigation on impact and bending properties of a novel dactyl-inspired sandwich honeycomb with carbon fiber. *Construction and Building Materials* 2020; 253: 119161.

64. Baran I and Weijermars W. Residual bending behaviour of sandwich composites after impact. *Journal of Sandwich Structures & Materials* 2020; 22: 402–422.
65. Afolabi OA, Kanny K and Mohan TP. Investigation of mechanical characterization of hybrid sandwich composites with syntactic foam core for structural applications. 2023; 32: 1–14.
66. Wu Z, Liu W, Wang L, et al. Theoretical and experimental study of foam-filled lattice composite panels under quasi-static compression loading. *Composites Part B: Engineering* 2014; 60: 329–340.
67. Hussain M, Abbas N, Zahra N, et al. Investigating the performance of GFRP/wood-based honeycomb sandwich panels for sustainable prefab building construction. *SN Appl Sci* 2019; 1: 1–8.
68. Al-Fasih MY, Kueh ABH and Ibrahim MHW. Flexural behavior of sandwich beams with novel triaxially woven fabric composite skins. *Steel Compos Struct* 2020; 34: 299–308.
69. Dhaliwal GS and Newaz GM. Flexural response of degraded polyurethane foam core sandwich beam with initial crack between facesheet and core. *Materials (Basel, Switzerland)* 2020; 13: 1–18.
70. Khaledi H and Rostamiyan Y. Flexural strength of foam-filled polymer composite sandwich panel with novel M-shaped core reinforced by nano-SiO 2. *Polymer Composites* 2021; 42: 6704–6718.
71. Pathan M V., Patsias S, Rongong JA, et al. Measurements and predictions of the viscoelastic properties of a composite lamina and their sensitivity to temperature and frequency. *Composites Science and Technology* 2017; 149: 207–219.
72. Pathan M V., Tagarielli VL and Patsias S. Effect of fibre shape and interphase on the anisotropic viscoelastic response of fibre composites. *Composite Structures* 2017; 162: 156–163.
73. Redmann A, Montoya-Ospina MC, Karl R, et al. High-force dynamic mechanical analysis of composite sandwich panels for aerospace structures. *Composites Part C: Open Access* 2021; 5: 100136. DOI: 10.1016/j.jcomc.2021.100136.
74. Richardson MOW and Wisheart MJ. Review of low-velocity impact properties of composite materials. *Composites Part A: Applied Science and Manufacturing* 1996; 27: 1123–1131.
75. Cantwell WJ and Morton J. The impact resistance of composite materials - a review. *Composites* 1991; 22: 347–362.
76. Joshi SP and Sun CT. Impact-induced fracture initiation and detailed dynamic stress field in the vicinity of the impact. In: American Society of Composites: Second Technical Conference, Tucson, AZ, USA, 19–21 September 2022.
77. Walsh J, Kim HI and Suhr J. Low velocity impact resistance and energy absorption of environmentally friendly expanded cork core-carbon fiber sandwich composites. *Composites Part A: Applied Science and Manufacturing* 2017; 101: 290–296.
78. Morada G, Ouadday R, Vadean A, et al. Low-velocity impact resistance of ATH/epoxy core sandwich composite panels: experimental and numerical analyses. *Composites Part B: Engineering* 2017; 114: 418–431.
79. Mezeix L, Dols S, Bouvet C, et al. Experimental analysis of impact and post-impact behaviour of inserts in Carbon sandwich structures. *Journal of Sandwich Structures & Materials* 2019; 21: 135–153.

80. Dabiryan H, Hasanalizade F and Sadighi M. Low-velocity impact behavior of composites reinforced with weft-knitted spacer glass fabrics. *Journal of Industrial Textiles* 2019; 49: 465–483.
81. Chen Y, Hou S, Fu K, et al. Low-velocity impact response of composite sandwich structures: modelling and experiment. *Composite Structures* 2017; 168: 322–334.
82. Bahei-El-Din Y, Shazly M and Salem S. *Impact Resistance of Sandwich Plates*. Amsterdam, Netherlands: Elsevier, 2016, pp. 471–489. DOI: 10.1016/b978-0-08-100080-9.00016-6.
83. Guan Z, He W, Chen J, et al. Permanent indentation and damage creation of laminates with different composite systems: an experimental investigation. *Polymer Composites* 2014; 35: 872–883. DOI: 10.1002/pc.22731.
84. Wagih A, Maimí P, Blanco N, et al. A quasi-static indentation test to elucidate the sequence of damage events in low velocity impacts on composite laminates. *Composites Part A: Applied Science and Manufacturing* 2016; 82: 180–189.
85. Eltaher MA, Alsulami R and Wagih A. On the evolution of energy dissipation in dispersed composite laminates under out-of-plane loading. *Composites Part B: Engineering* 2021; 216: 108864. DOI: 10.1016/j.compositesb.2021.108864.
86. Almitani KH, Wagih A, Melaibari A, et al. Improving energy dissipation and damage resistance of CFRP laminates using alumina nanoparticles. *Plastics, Rubber and Composites* 2019; 48: 208–217.
87. Abisset E, Daghia F, Sun XC, et al. Interaction of inter- and intralaminar damage in scaled quasi-static indentation tests: Part 1 - Experiments. *Composite Structures* 2016; 136: 712–726.
88. Wagih A, Maimí P, González EV, et al. Damage sequence in thin-ply composite laminates under out-of-plane loading. *Composites Part A: Applied Science and Manufacturing* 2016; 87: 66–77.
89. Du L and Jiao G. Indentation study of Z-pin reinforced polymer foam core sandwich structures. *Composites Part A: Applied Science and Manufacturing* 2009; 40: 822–829.
90. Sutherland LS and Guedes Soares C. The use of quasi-static testing to obtain the low-velocity impact damage resistance of marine GRP laminates. *Composites Part B: Engineering* 2012; 43: 1459–1467.
91. Raju KS, Smith BL, Tomblin JS, et al. Impact damage resistance and tolerance of honeycomb core sandwich panels. *Journal of Composite Materials* 2008; 42: 385–412.
92. Daniel IM, Abot JL, Schubel PM, et al. Response and damage tolerance of composite sandwich structures under low velocity impact. *Experimental Mechanics* 2012; 52: 37–47.
93. Schubel PM, Luo JJ and Daniel IM. Impact and post impact behavior of composite sandwich panels. *Composites Part A: Applied Science and Manufacturing* 2007; 38: 1051–1057.
94. Zhu F, Lu G, Ruan D, et al. Plastic deformation, failure and energy absorption of sandwich structures with metallic cellular cores. *International Journal of Protective Structures* 2010; 1: 507–541.
95. Abrate S. *Impact Energy of cComposite Structures. Course and*. illinois, USA: International Centre for Mechanincal Sciences, 2011.
96. Zhu F, Wang Z, Lu G, et al. Some theoretical considerations on the dynamic response of sandwich structures under impulsive loading. *International Journal of Impact Engineering* 2010; 37: 625–637.

97. Rubino V, Deshpande VS and Fleck NA. The dynamic response of clamped rectangular Y-frame and corrugated core sandwich plates. *European Journal of Mechanics - A/Solids* 2009; 28: 14–24.
98. Tilbrook MT, Deshpande VS and Fleck NA. Underwater blast loading of sandwich beams: regimes of behaviour. *International Journal of Solids and Structures* 2009; 46: 3209–3221.
99. Brekken KA, Reyes A, Børvik T, et al. Sandwich panels with polymeric foam cores exposed to blast loading: An experimental and numerical investigation. *Appl Sci* 2020; 10: 1–36.
100. Wang D. Impact behavior and energy absorption of paper honeycomb sandwich panels. *International Journal of Impact Engineering* 2009; 36: 110–114.
101. Tao Q, Ren P, Shi L, et al. Energy absorption and impact behavior of composite sandwich panels under high-velocity spherical projectile. *International Journal of Impact Engineering* 2022; 162: 104143.
102. Ivañez I, Sánchez-Saez S, Garcia-Castillo SK, et al. High-velocity impact behaviour of damaged sandwich plates with agglomerated cork core. *Composite Structures* 2020; 248: 112520. DOI: 10.1016/j.compstruct.2020.112520.
103. Ahmadi E, Atrian A, Fesharaki JJ, et al. Experimental and numerical assessment of high-velocity impact behavior of syntactic foam core sandwich structures. *European Journal of Mechanics - A/Solids* 2021; 90: 104355.
104. Usta F, Türkmen HS and Scarpa F. High-velocity impact resistance of doubly curved sandwich panels with re-entrant honeycomb and foam core. *International Journal of Impact Engineering* 2022; 165: 104230.
105. Han F, Yan Y and Ma J. Experimental study and progressive failure analysis of stitched foam-core sandwich composites subjected to low-velocity impact. *Polymer Composites* 2018; 39: 624–635.
106. Zhang X, Xu F, Zang Y, et al. Experimental and numerical investigation on damage behavior of honeycomb sandwich panel subjected to low-velocity impact. *Composite Structures* 2020; 236: 111882.
107. Ghalami-Choobar M and Sadighi M. Investigation of high velocity impact of cylindrical projectile on sandwich panels with fiber-metal laminates skins and polyurethane core. *Aerospace Science and Technology* 2014; 32: 142–152.
108. Ahmadi H, Liaghat GH, Sabouri H, et al. Investigation on the high velocity impact properties of glass-reinforced fiber metal laminates. *Journal of Composite Materials* 2013; 47: 1605–1615.
109. Aryal B, Morozov EV and Shankar K. Effects of ballistic impact damage on mechanical behaviour of composite honeycomb sandwich panels. *Journal of Sandwich Structures & Materials* 2021; 23: 2064–2085.
110. Naghizadeh Z, Faezipour M, Hossein Pol M, et al. High velocity impact response of carbon nanotubes-reinforced composite sandwich panels. *Journal of Sandwich Structures & Materials* 2020; 22: 303–324.
111. Ni CY, Hou R, Xia HY, et al. Perforation resistance of corrugated metallic sandwich plates filled with reactive powder concrete: experiment and simulation. *Composite Structures* 2015; 127: 426–435.

112. Mei J, Liu J, Zhang M, et al. Experimental and numerical study on the ballistic impact resistance of the CFRP sandwich panel with the X-frame cores. *International Journal of Mechanical Sciences* 2022; 232: 107649.
113. Studziński R and Pozorski Z. Experimental and numerical analysis of sandwich panels with hybrid core. *J Sandw Struct Mater* 2018; 20: 271–286.
114. Marannano G and Zuccarello B. Analysys and optimization of an end double-lap bonded joint for GFRP composite sandwich panels. *Journal of Sandwich Structures & Materials* 2022; 24: 2153–2177.
115. Gouskos D and Iannucci L. A failure model for the analysis of cross-ply Non-Crimp Fabric (NCF) composites under in-plane loading: experimental & numerical study. *Engineering Fracture Mechanics* 2022; 271: 108575.
116. Wang H, Ramakrishnan KR and Shankar K. Experimental study of the medium velocity impact response of sandwich panels with different cores. *Materials & Design* 2016; 99: 68–82.
117. Delavari K and Dabiryan H. Mathematical and numerical simulation of geometry and mechanical behavior of sandwich composites reinforced with 1 × 1-Rib-Gaiting weft-knitted spacer fabric; compressional behavior. *Composite Structures* 2021; 268: 113952.
118. Berggreen C and Simonsen BC. Non-uniform compressive strength of debonded sandwich panels - II. Fracture mechanics investigation. *Journal of Sandwich Structures & Materials* 2005; 7: 483–517. DOI: 10.1177/1099636205054790.
119. Moslemian R and Berggreen C. Interface fatigue crack propagation in sandwich X-joints - Part II: finite element modeling. *Journal of Sandwich Structures & Materials* 2013; 15: 451–463.
120. Martakos G, Andreasen JH, Berggreen C, et al. Interfacial crack arrest in sandwich panels with embedded crack stoppers subjected to fatigue loading. *Applied Composite Materials* 2017; 24: 55–76.
121. Ivañez I, Santiuste C and Sanchez-Saez S. FEM analysis of dynamic flexural behaviour of composite sandwich beams with foam core. *Compos Struct* 2010; 92: 2285–2291.
122. Zhao D, Liu TQ, Lu X, et al. Experimental and numerical analysis of a novel curved sandwich panel with pultruded GFRP strip core. *Composite Structures* 2022; 288: 115404.
123. Peliński K and Smardzewski J. Static response of synclastic sandwich panel with auxetic wood-based honeycomb cores subject to compression. *Thin-Walled Struct* 2022; 179: 109559.
124. Hashin Z. Failure criteria for unidirectional fiber composites. *Journal of Applied Mechanics* 1980; 47: 329–334.
125. Hashin Z and Rotem A. A fatigue failure criterion for fiber reinforced materials. *Journal of Composite Materials* 1973; 7: 448–464.
126. Hohe J, Hardenacke V, Fascio V, et al. Numerical and experimental design of graded cellular sandwich cores for multi-functional aerospace applications. *Materials & Design* 2012; 39: 20–32.
127. Foo CC, Seah LK and Chai GB. A modified energy-balance model to predict low-velocity impact response for sandwich composites. *Composite Structures* 2011; 93: 1385–1393.

128. He W, Wu J, Yao L, et al. Numerical investigation of dynamic response and failure mechanisms for composite lattice sandwich structure under different slamming loads. *Applied Composite Materials* 2021; 28: 1477–1509. DOI: 10.1007/s10443-021-09919-6.
129. Liu N, Ren X and Lua J. An isogeometric continuum shell element for modeling the nonlinear response of functionally graded material structures. *Composite Structures* 2020; 237: 111893.
130. Liu N and Jeffers AE. Isogeometric analysis of laminated composite and functionally graded sandwich plates based on a layerwise displacement theory. *Composite Structures* 2017; 176: 143–153.
131. *Abaqus Benchmarks Guide*. Seattle, WA: University of Washington.
132. Calabrese L, Fiore V, Scalici T, et al. Experimental assessment of the improved properties during aging of flax/glass hybrid composite laminates for marine applications. *J Appl Polym Sci* 2019; 136: 1–12.
133. Park Y Bin, Kweon JH and Choi JH. Failure characteristics of carbon/BMI-Nomex sandwich joints in various hygrothermal conditions. *Composites Part B: Engineering* 2014; 60: 213–221.
134. Le Duigou A, Davies P and Baley C. Seawater ageing of flax/poly(lactic acid) biocomposites. *Polymer Degradation and Stability* 2009; 94: 1151–1162.
135. Dezulier Q, Clement A, Davies P, et al. Water ageing effects on the elastic and viscoelastic behaviour of epoxy-based materials used in marine environment. *Composites Part B: Engineering* 2022; 242: 110090.
136. Dhakal HN, Zhang ZY and Richardson MOW. Effect of water absorption on the mechanical properties of hemp fibre reinforced unsaturated polyester composites. *Composites Science and Technology* 2007; 67: 1674–1683.
137. Obeid H, Clément A, Fréour S, et al. On the identification of the coefficient of moisture expansion of polyamide-6: accounting differential swelling strains and plasticization. *Mechanics of Materials* 2018; 118: 1–10.
138. Quino G, Tagarielli VL and Petrinic N. Effects of water absorption on the mechanical properties of GFRPs. *Composites Science and Technology* 2020; 199: 108316. DOI: 10.1016/j.compscitech.2020.108316.
139. Chakraverty AP, Mohanty UK, Mishra SC, et al. Sea water ageing of GFRP composites and the dissolved salts. In: IOP Conference Series: Materials Science and Engineering, Rourkela, India, 5–6 December 2014. DOI: 10.1088/1757-899X/75/1/012029.
140. Kane SN, Mishra A and Dutta AK. International conference on recent trends in physics 2016 (ICRTP2016). *Journal of Physics: Conference Series* 2016; 755: 011001. DOI: 10.1088/1742-6596/755/1/011001.
141. Li H, Zhang K, Fan X, et al. Effect of seawater ageing with different temperatures and concentrations on static/dynamic mechanical properties of carbon fiber reinforced polymer composites. *Composites Part B: Engineering* 2019; 173: 106910. DOI: 10.1016/j.compositesb.2019.106910.
142. Rizov VI. Elastic-plastic response of structural foams subjected to localized static loads. *Materials & Design* 2006; 27: 947–954.

143. Gupta N and Woldesenbet E. Hygrothermal studies on syntactic foams and compressive strength determination. *Composite Structures* 2003; 61: 311–320.
144. Tagliavia G, Porfiri M and Gupta N. Influence of moisture absorption on flexural properties of syntactic foams. *Composites Part B: Engineering* 2012; 43: 115–123.

Appendix

Acronyms

CAI	Compression after impact
CDM	Continuum damage mechanics
CFRP	Carbon-fibre-reinforced plastics
DCB	Double Cantilever Beam
DSH	Dactyl-inspired sandwich-structural honeycomb
FEA	Finite Element Analysis
FRP	Fibre-reinforced plastics
GFRP	Glass-fibre-reinforced plastics
PET	Polyethylene terephthalate
PSH	Plain-woven skin sandwich-structural honeycomb
PVC	Polyvinyl chloride
QSI	Quasi-static indentation
SEA	Specific Energy Absorption
USH	Unidirectional Skin-sandwich structural honeycomb